Reference: *Biol. Bull.*, 159: 376–393. (October, 1980)

ELECTRICAL ACTIVITIES IN THE SUBTENTACULAR REGION OF THE ANTHOMEDUSAN *SPIROCODON SALTATRIX* (TILESIUS)

KOHZOH OHTSU

Ushimado Marine Laboratory, Okayama University, Kashino, Ushimado, Oku, Okayama, 701-43 Japan

Electrophysiological studies of hydrozoans have revealed various kinds of electrical pulses of epithelial, muscular, or nervous origin. One striking feature of hydrozoans is that the conducting systems of those pulses often lie parallel to one another. It is interesting to determine how such parallel systems function and therefore, much effort has been made to show the origin, nature, and function of each conducting system, *e.g.*, in *Hydra* (Passano and McCullough, 1962, 1964, 1965; Josephson and Macklin, 1967; Josephson, 1967; Macklin and Josephson, 1971; Rushforth and Burke, 1971; Rushforth, 1971), in *Tubularia* (Josephson and Mackie, 1965; Josephson, 1965, 1974; Josephson and Rushforth, 1973; Kruijf, 1977), in hydromedusans (Spencer, 1975, 1978; Mackie, 1975) and in siphonophores (Mackie, 1976a, 1978). *Spirocodon*, the hydrozoan medusa used in this study, also has such parallel systems in some tissues (Ohtsu and Yoshida, 1973). Only those in the area between the ocelli and the nerve ring called the "subtentacular region" will be considered here.

Spirocodon saltatrix has many morphological charactristics in common with other species of Anthomedusae (Horridge, 1955; Mackie and Passano, 1968; Spencer, 1979; King and Spencer, 1979); but it shows some striking differences from them in the marginal region of the umbrella.

Figure 1 shows a part of the subtentacular region. According to Uchida (1927), the subtentacular region is formed in the following manner: In early developmental stages, single ocelli are present at the base of the four perradial and the four interradial tentacles, close to the nerve rings. As tentacles grow, these ocelli move away from the inner margin of the umbrella, forming an intervening expanse of tentacular tissues, the radial streaks, between the ocelli and the nerve ring while new ocelli and tentacles are formed at both sides of and slightly below those already formed. The newer the ocelli, the shorter the radial streaks. Thus a crescent-like area called the subtentacular region is produced between the ocelli (tentacular bases) and the nerve rings (velar base). A fully grown medusa has eight subtentacular regions at the lower margin of the umbrella. In large specimens, each subtentacular region contains more than 60 radial streaks. Sketches of the subtentacular region and the whole body are shown in Ohtsu and Yoshida (1973).

The subtentacular region should provide pathways for excitations traveling from the periphery (tentacles and ocelli) to the center (nerve ring). Histological as well as electrophysiological investigations were carried out to identify cell types within the subtentacular region in order to provide a morphological basis for interpreting data on pulse generating sites characterizing each conducting system.

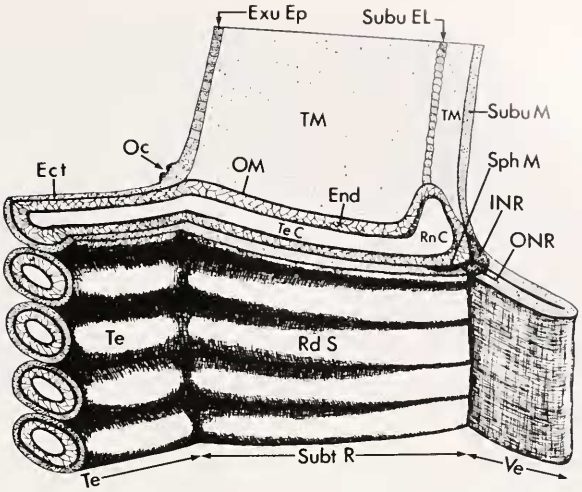

FIGURE 1. The subtentacular region. Four and a half radial streaks are shown. Ect, ectoderm; End, endoderm; Exu EP, exumbrellar epithelium; INR, inner nerve ring; TM, transparent mesogloea; Oc, ocellus; ONR, outer nerve-ring; Rd S, radial streak; Rn C, ring canal; Sph M, marginal sphincter muscle; Subt. R, subtentacular region; Subu EL, subumbrellar endodermal lamella; Subu M, subumbrellar muscle sheet; Te, tentacle; Te C, tentacular canal; OM, opaque mesogloea; Ve, velum. For explanation, see text.

MATERIALS AND METHODS

Specimens of *Spirocodon saltatrix* were collected from the Seto Inland Sea, Japan, and kept in running sea water. Half of the subtentacular region, with a small fraction of mesogloea lying under it, was dissected from the margin of the umbrella and used for histological observations and electrical recordings.

For electron- and light-microscopical observations, the ocelli and radial streaks were dissected from the subtentacular region. They were fixed in chilled 2% glutaraldehyde for 2 hr and post-fixed in 2% osmium tetroxide for 2.5 hr. To regulate osmolarity, 0.9 M sucrose or sea water was used. In some cases, fixation was done at 15°C for the first hour to retain microtuble structure. Fixatives were buffered with 0.1 M Na-cacodylate, pH 8.0. Post-fixation was omitted in the dye-marking experiment described later. The specimens were dehydrated through an ethanol series and embedded in TAAB embedding resin (TAAB Laboratories). Sections were cut with a Porter-Blum MT-2B ultramicrotome. Silver to gray sections were stained with uranyl acetate and then lead citrate and observed with a Hitachi electron microscope (HS-8). Thicker sections of 1–2 μm were stained with methylene blue for light microscopy.

Experiments were performed at room temperature (18–21°C). The arrangement of the recording chamber was similar to that described in Ohtsu and Yoshida (1973). During recording, the surface of the preparation was exposed to air to reduce short-circuit currents. During intracellular recording, preparations were almost totally immersed in sea water. Recording electrodes were advanced with a hydraulic micromanipulator in conjunction with a mechanical advance.

For extracellular recordings, two types of glass micropipette electrodes were used: rigid or floating. The latter consisted of a coiled piece of tungsten wire (30 μm diameter) joined with wax to the proximal opening of a micropipette electrode tip a few millimeters long. This type of electrode allowed vigorous move-

ments of the preparation without electrical artifacts. Both types of electrodes were filled with sea water. External tip diameters ranged from 1 to 5 μm.

For intracellular recordings, micropipettes were filled with 2 M KCl and had DC-resistances of 20–100 MΩ. Rigid electrodes were used. Preparations were treated with a 0.3–0.5% pronase/sea-water solution for 4–8 min to facilitate penetration, aided by a jolting device (Tomita *et al.*, 1967).

A 1–2 hr immersion in pronase was used to dissociate the endodermal cells for examination with Normarski optics (Leitz, Orthoplan).

To measure depth of penetration of the recording electrode tips, a pair of electrodes was used, unless stated otherwise. Initially, both electrodes were placed on the surface of the radial streak and then one electrode was advanced through the tissues, leaving the other on the surface. Because smooth penetration was impossible, depths were estimated during withdrawal of the electrode, using a micromanipulator scale.

A micropipette filled with M/2 K-ferrocyanide instead of sea water was used to mark the recording sites. The pipettes with K-ferrocyanide were not used as recording electrodes because leakage of the electrolyte from the large pipette tips might have deleterious effects and because tissue penetration with such pipettes often resulted in failure of electrophoretic ejection of the fluid, probably because the pipette tips became plugged with tissue debris during penetration. After recording, the pipette with K-ferrocyanide was attached to the recording electrode tip and the electrolyte was expelled into tissues by inonophoretic current. One or two drops of ferric chloride solution were delivered to make a Berlin blue precipitate. Cross-sectional dimensions of tissues were estimated from light micrographs compared with readings from the micromanipulator scale.

The most serious difficulty with the rigid electrode was immobilizing the preparations. Since tissues can contract locally, mechanical restraint was impossible. Instead, various anaesthetics, such as urethane, menthol, MS-222, and magnesium chloride, were tried. Urethane was most successful. The urethane concentration was varied within the range of $1.0–3.0 \times 10^{-1}$ M, since the effect was not the same on every preparation.

Pulses can be evoked by termination of adapting light (Ohtsu and Yoshida, 1973). Light from a tungsten lamp (35 W) was delivered through a heat-absorbing filter and a light guide, the illuminance of which was 3500 lux in the plane of the preparation.

Electrical stimulation was by means of paired silver wires of 200 μm diameter through an isolation unit (Nihon Kohden, MSE-JM). In some cases, however, stimuli were delivered through the recording electrode.

Electrical responses were fed to a two-channel preamplifier formed by two FET-coupled operational amplifiers (Teldyne Filbrick, 142502) arranged in parallel. One was equipped with a Wheatstone bridge circuit, permitting measurement of membrane resistance changes. Two DC/AC amplifiers (Nihon Kohden, AVM-9S, AVH-9) were employed; the former, equipped with a beam chopper device, was most frequently used. The latter was used as a differential amplifier or to monitor photosignals. All responses were displayed on a dual-beam cathode ray oscilloscope (Nihon Kohden, VC-9A), photographed by a continuous recording camera (Nihon Kohden, PC-2B) and visually monitored on a second oscilloscope (Iwatsu, SS-5100).

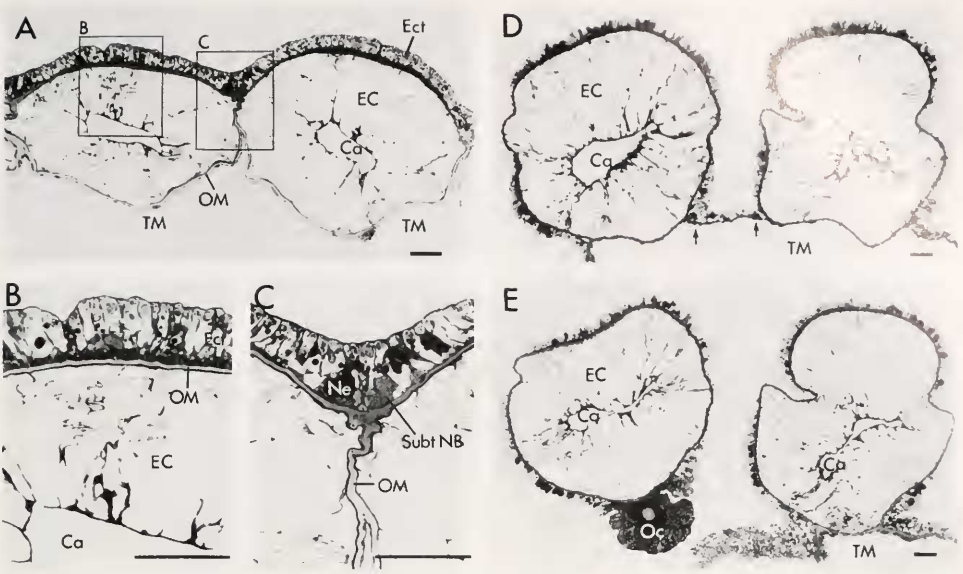

FIGURE 2. Photomicrographs of cross-sections through the radial streaks. Ca, canal; EC, endodermal cell; Ect, ectoderm; Ne, nematocyst; Oc, ocellus; OM, opaque mesogloea; Subt NB, subtentacular nerve bundle; TM, transparent mesogloea. Arrows in D show the subtentacular nerve bundles. Horizontal bars, 50 μm.

RESULTS

Histological observations

The ectoderm of the radial streaks is similar to that of the tentacles of other hydromedusans. Figure 2A shows a cross-section of two radial streaks. Figures 2B and C show enlargements of parts of A. Endodermal epithelial cells, surrounding the tentacular canal situated at the center, project their fine cytoplasmic processes towards a surrounding thin mesogloeal layer, resulting in many large endodermal spaces separated by the processes. The endodermal spaces may look larger in the photomicrographs than they actually are (Fig. 2) because the fine endodermal processes are often smaller than 0.1 μm, and thus beyond the limit of resolution of the light microscope. The mesogloeal layer is far more opaque than the jelly-like mesogloea found elsewhere. Therefore it will be called the opaque mesogloea and the latter, the transparent mesogloea. A layer of ectodermal cells surrounds the opaque mesogloea. The transparent mesogloea cannot be seen because it has the same refractive index as the embedding resin.

The subtentacular region is folded between adjacent radial streaks, forming a groove (Fig. 2A) where a single nerve bundle runs (Fig. 2C). This bundle will be called a subtentacular nerve bundle. The grooves become flatter near the nerve-rings. In contrast, going towards the ocelli away from the nerve-rings, the grooves become deeper, *i.e.,* the ectodermal cell layer extends progressively around the endoderm, while the subtentacular nerve bundle divides into two branches, each running in a corner of the groove (Fig. 2D). When the ectoderm completely surrounds the endoderm, the ocelli appear in the ectoderm on the exumbrellar side (Fig. 2E). Beyond the ocelli, the radial streaks become the tentacles.

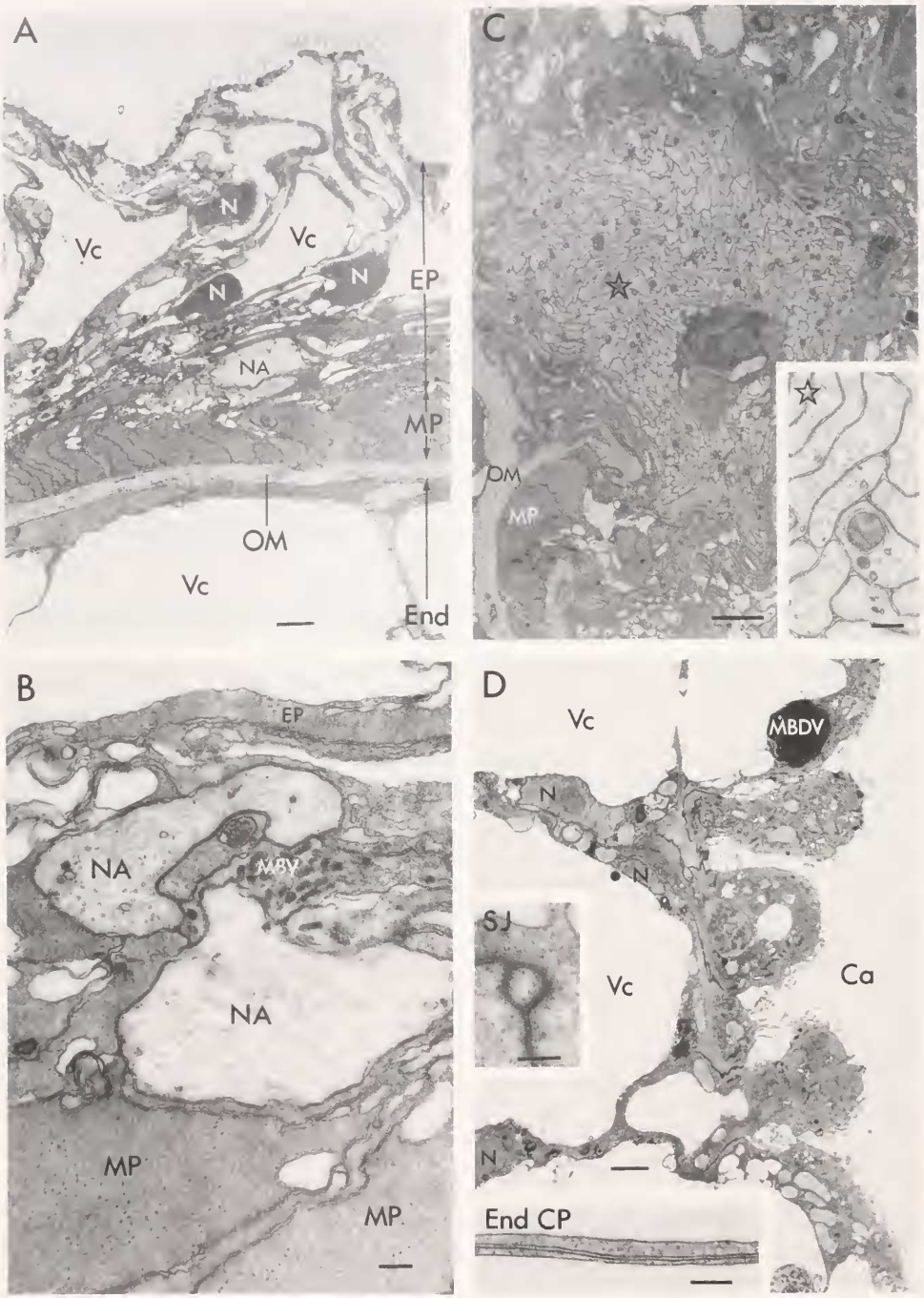

FIGURE 3. Electron micrographs of cross-sections through the radial streaks. A, the ectoderm and a part of the endoderm; B, high magnification of the endoderm; C, the subtentacular nerve bundle and high magnification of a part of it (asterisk); D, endodermal cells. Ca, canal; End, endoderm; End CP, fine endodermal cell process; EP, the epithelial process of the myoepithelial cell; MBV, membrane bound vesicle; MBDV, membrane bound digestive

The construction of the tentacles, therefore, necessarily resembles that of the radial streaks. In the vicinity of the ocelli, the nerve bundles are missing, probably because the nerves have dispersed. It seems that at least some axons, if not all of them, receive input from the ocelli and function in the photoresponse. The major functions of the subtentacular nerve bundle, however, are unknown.

Figures 3A-C show the ultrastructure of the ectoderm in cross sections. The thickness of the layer usually lies in the range 10–50 μm though it varies in different preparations and in different parts of the sections. The muscular processes of the myoepithelial cells are smooth muscle fibers running along the axis of the tentacle. They lie in a layer on the innermost side of the ectoderm, anchored to the mesogloea (A). They are connected with each other by structures resembling the gap junctions reported in other hydrozoan cells (Hand and Gobel, 1972). The muscle layer becomes thinner towards the nerve-ring and thicker towards the tentacle. The epithelial proccesses lying at the outermost surface and forming almost the whole surface of the ectoderm contain the nuclei and extremely large vacuoles lying in relatively undifferentiated cytoplasm (A). The opaque mesogloea is perforated in places by a tissue similar to that of the endodermal cell processes, allowing direct contact between the ectoderm and the endoderm, as reported in other anthomedusans (Boelsterli, 1977).

A number of nerve axons with variable diameters (Figs. 3A, B) and sometimes neuronal somata of about 5–10 μm in diameter are present. Both contain a number of microtubules and often membrane-bound vesicles. They are almost always adjacent to the myoepithelial cells. Some cells with a number of membrane-bound vesicles (recalling neurosecretory granules), are also observed (Fig. 3B). Synapse-like structures, however, have not been found so far between the cells identified, though they are frequently observed around the ocelli (Toh *et al.*, 1979).

The subtentacular nerve bundles consist of a large number of fine axons which contain many microtubules and membrane-bound vesicles (Fig. 3C). The number of axons differs from preparation to preparation but gradually decreases going towards the ocelli. No neuronal somata have so far been found along the bundle. They probably lie elsewhere, *e.g.*, adjacent to the ocelli or outside the nerve bundle. It must be noted that muscle processes are weakly developed near the subtentacular nerve bundle.

Cnidocytes are also present among the myoepithelial cells in the subtentacular region but they are far less abundant than in the tentacles.

The fine structure of the endodermal epithelial cells is shown in Figure 3D. A single type of endodermal cell can be identified in the subtentacular region except near the ring canal, where endodermal nerves can be seen as reported in *Stomotoca* (Mackie and Singla, 1975) and *Polyorchis* (Singla, 1978; Spencer, 1979). The endodermal cell cytoplasm expands on the side facing the tentacular canal, and the endoplasmic reticulum, Golgi apparatus, and mitochondria are in this region. A number of microvilli and cilia are present on the surface adjacent to the canal. Septate desmosomes are also observed connecting cells on their lumenal sides (Fig. 3D, inset). Membrane-bound digestive vacuoles are often observed, suggesting active phagocytosis. The nuclei lie towards the periphery. More peripherally, the cell processes become thin but often form enlargements including mitochondria and even nuclei on occasion, and extending in sheets of two

vacuole; MP, the myonal process of the myoepithelial cell; N, nucleus; NA, nerve axon; OM, opaque mesogloea; SJ, septate junction; Vc, vacuole. Horizontal bars, 0.2 μm in C and D insets and 2 μm in the others.

or more layers as far as the opaque mesogloea, creating many large spaces between the cell processes (Figs. 2, 3A, 3D inset). Where they reach the opaque mesogloea, the epithelial cell processes line its inner side (Fig. 3A).

Although the large endodermal spaces seen among the epithelial cell processes appear to be extracellular, this may not be the case. The epithelial process almost always consists of at least two layers of endoderm (Fig. 3D, inset). The narrow gap between the two layers is extracellular space, often observed to be connected with the central canal via a septate junction. If the large endodermal spaces were extracellular spaces, then they, too, should often be connected to the canal. But such cases have not been observed in electron micrographs. It is likely, therefore, that the large endodermal spaces represent extraordinarily large vacuoles in endodermal epithelial cells. Supporting evidence was obtained from experiments involving dissociation of the tissues with pronase. As the endodermal cells dissociate, the endodermal spaces become spherical and some of the cells break free as single spherical cells. Vacuoles occupy the greater part of the cytoplasm and the nuclei and major portion of the cytoplasm lie near the periphery of the cell. Cells isolated from the endoderm vary greatly in size. For instance, in one treatment the cells measured 15–20 μm and sometimes 30 μm, but in another treatment some cells measured 100 μm.

Conduction velocities of pulses recorded

When the recording electrode is placed at the surface of the subtentacular region, three types of pulses are recorded: slow monophasic pulses (SMPs; Figs. 4A, C), quick and slow compound pulses (QSCPs; Figs. 4A–D), and tentacle contraction pulses (TCPs; Fig. 4D). The first two were reported by Ohtsu and Yoshida (1973). The QSCP consists of a very short phase preceding a slow

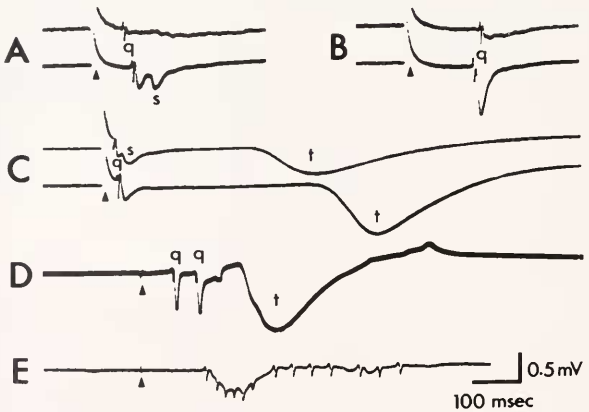

FIGURE 4. Pulses recorded in the subtentacular region. A and B show conduction of QSCPs. In A, a single electrical stimulus was delivered to a part of a tentacle distal to the recording sites. In B, a stimulus was delivered to an adjacent tentacle. C shows TCPs (t) following long after QSCPs and an SMP. D shows a TCP (t) following soon after two successive QSCPs, suggesting triggering of the TCP by the QSCPs. The distance between the recording electrodes and the stimulus site is much larger in D than C, as can be seen from the longer delay of the QSCPs after the electrical stimulus. E shows multiple firing of the quick phase of QSCPs over the course of the prolonged slow phase induced by urethane treatment. Arrows, electrical stimuli. "q" and "s" indicate a QSCP (or QSCPs) and an SMP, respectively.

phase which bears a remarkable resemblance to the SMP in terms of its time course and waveform (Fig. 4A).

A preliminary experiment showed that the conduction velocity of QSCPs in the subtentacular region is approximately 60 cm/sec (Ohtsu and Yoshida, 1973). This value represented only a single measurement, however, so further detailed bidirectional measurements were performed on the tentacles, taking advantage of their greater length. Electrical stimuli were employed to evoke QSCPs. At proximal parts of moderately relaxed tentacles, conductive velocities were calculated from the time difference between the quick components of the QSCPs recorded at two recording electrodes. For distal to proximal conduction, stimuli were delivered at distal parts of the tentacles with recording electrodes placed more proximally (Fig. 4A), while for proximal to distal conduction a neighboring tentacle was stimulated (Fig. 4B). In the latter case, QSCPs would first travel proximally up the stimulated tentacle and would reach the recording sites by travelling distally down the second tentacle after crossing the subtentacular region. The longer post-stimulus delays of the pulses in Figure 4B, compared with those in Figure 4A, reflect the longer distance travelled. The mean value obtained from 25 different tentacles from eight animals was 75 cm/sec (range, 50–104 cm/sec) in distal to proximal direction and 73 cm/sec (range, 57–95 cm/sec) in the opposite direction. In most cases, QSCPs appeared coupled with each other on a one-to-one basis within the subtentacular region and the tentacles associated with it.

SMPs can be conducted for only a short distance within the same radial streak (Ohtsu and Yoshida, 1973). The generating sites of spontaneously occurring SMPs frequently changed, as shown in Figure 7A, where with the first SMP pair, a pulse first appears on the lower trace and then on the upper trace, while in the second pair, pulses appear in the reverse order. Moreover, SMPs sometimes disappeared between the two electrodes and were not conducted (Fig. 4C). Although the pulses can be induced by termination of adapting light with latencies of 0.2–1.1 sec, probably mediated by the ocelli (Ohtsu and Yoshida, 1973), it was difficult to restrict pulse generation to a single fixed site; one should be cautious in estimating the conduction velocity because the pulses were often generated between two recording electrodes. Waveforms of SMPs became variable as they moved distally along the tentacles so that it was often difficult to identify the corresponding phases of pulses recorded at two points. Estimation of conduction velocity, therefore, was performed in the subtentacular region, using spontaneous pulses or pulses triggered by lights-off and measuring the peak-to-peak time delay, since the initial rising phase was not steep enough to allow initiation time to be accurately determined. Cases with extremely short time delays were excluded, as they were probably due to initiation of pulses between the two recording electrodes. The mean value from 32 different radial streaks from eight animals was 16 cm/sec (range, 9–38 cm/sec). It must be noted that SMPs with conduction velocities less than 9 cm/sec were seen, especially during sequences where later pulses tended to be conducted far more slowly than earlier ones. However, these data were omitted from the above measurements, since they were obtained in experiments using urethane. There may be more than one conducting pathway for SMPs.

When electrical recordings were performed on the subtentacular region or the tentacles, extremely slow deflections with monophasic and sometimes more complicated waveforms were observed, accompanied by muscle contractions (Fig. 4C); the waveforms may include electrical artifacts due to tentacular movements. These pulses are referred to hereafter as tentacle contraction pulses (TCPs).

Measurement of their conduction velocity was done as for SMPs but using pulses elicited by electrical stimulation on the tentacles and recorded in the subtentacular region. Recordings were not made on the tentacles because the pulses were larger and of simpler waveform on the subtentacular region. The mean value from 29 different radial streaks from nine animals (range, 2.2–8.6 cm/sec), which is very slow compared with the conduction velocity of other pulses, suggests that TCPs are conducted without involvement of the nervous system. Figure 4C illustrates the great difference in the conduction velocities of QSCPs and TCPs, whereas the TCP in Figure 4D occured shortly after the QSCPs. A possible explanation for this is that TCPs can be induced directly by QSCPs in the course of conduction. Such examples, indicating triggering of TCPs, were often encountered when QSCPs appeared in rapid succession.

Waveform changes of pulses associated with electrode insertion depth

To determine where QSCPs originate, one of a pair of recording electrodes was inserted into a radial streak, while the other was placed on the surface. Urethane at 2×10^{-1} M concentration was used to immobilize the preparation although this concentration of urethane did not always completely abolish movement. This treatment, however, often prolonged the duration of the slow phase of QSCPs considerably and sometimes resulted in multiple firing of the quick phase over the course of the slow phase (Fig. 4E). This was never seen in untreated preparations.

Immobile preparations with normal pulse waveforms were selected for these experiments. Treatment with urethane further abolished the lights-off evocation of QSCPs and SMPs so that the pulses had to be evoked by electrical stimulation of distal parts of the tentacles, resulting in the disappearance of locally conducted SMPs.

During insertions of recording electrodes into the radial streak, smooth penetration was always interrupted in two places, once near the surface and again at considerable depth. The depths at which these interruptions occurred seem to correspond to the interfaces between the ectoderm and opaque mesogloea near the surface, and between the opaque and transparent mesogloea on the opposite side of the radial streak (see Fig. 2).

Results of one penetration experiment are shown in Figure 5: When both recording electrode tips were placed side by side on the surface of a radial streak, QSCPs with the same waveform appeared in the upper and the middle traces, with no deflection in the differential, lower trace (A). At a depth of 635 μm, a very small deflection with a waveform similar to that of the upper trace was observed (B). It must be noted, however, that in B and also in the following records, the pulses recorded on the surface were smaller than the one in A, presumably due to damage to cells near the surface by the electrode as it advanced and as the wider part of tapered electrode tip entered the surface tissues. Withdrawal of the electrode in 70 μm steps resulted in reversal of the polarity of the deflection in the middle trace (C). As the electrode was withdrawn further, positivity of the middle trace was gradually increased (D, E) and reached a maximum in or near the canal (F–H). With further withdrawal the slow deflection gradually became less positive (I–K) and eventually reversed its polarity again (L). Approaching still close to the surface, the negative slow deflection grew larger (M, N) and reached its maximum amplitude on the ectodermal surface (O). These facts clearly indicate that the surface of the radial

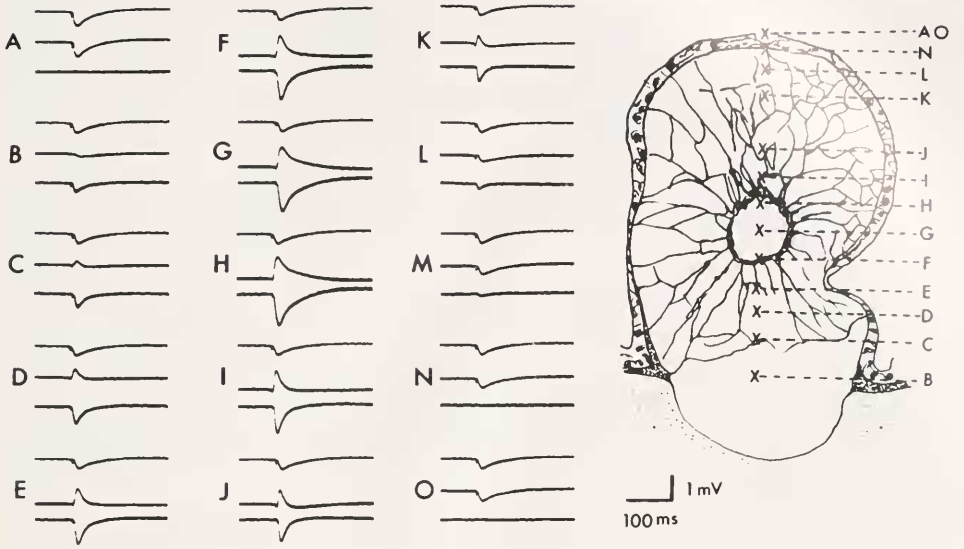

FIGURE 5. Waveform changes of QSCPs associated with the depth of the recording electrode tip. The recording electrode was inserted into the radial streak to a depth of 700 μm and then withdrawn stepwise. The upper traces were recorded from the surface electrode, the middle traces from the inserted electrode, and the lower traces show differential recordings (upper records minus middle records). The right inset diagram shows a cross-section of the radial streak used here. A, surface; B, 635 μm; C, 565 μm; D, 515 μm; E, 465 μm; F, 415 μm; G, 365 μm; H, 315 μm; I, 265 μm; J, 215 μm; K, 115 μm; L, 65 μm; M, 45 μm; N, 25 μm O, surface. QSCPs were evoked by electrical stimuli before initiation of the recordings.

streaks becomes negative (about 1.3 mV in H) compared with the central region of the endodermal canal during the slow phase of QSCPs. Similar results were obtained in four other preparations. Difference in DC-level measured between the ectoderm and the endoderm was variable, but in most cases was endodermal-side positive by a few millivolts.

The polarity of the quick phase of QSCPs, on the other hand, remained unchanged throughout the experiment. The amplitude was very small deep in the radial streak (Fig. 5B–J) and became larger when the electrode was moved to 100 μm or less from the surface (K–O). These changes are shown more clearly in Figure 6, where the quick phases were much larger than the slow phases, indicating that the recording site was nearer the nerve ring than the ocelli. The quick phases of QSCPs usually dominated the slow phase near the nerve ring, and vice versa near the ocelli; more nervous elements could be found near the former. Both the quick and slow phases of QSCPs abruptly increased when the electrode was withdrawn to within 40 μm of the surface of the ectoderm, strongly suggesting that both phases of QSCPs originate in the ectoderm. The waveforms of the pulses in Figure 6E closely resemble those at the surface (Fig. 6A) and such waveforms were often encountered when electrode tips obviously passed from the endoderm into the transparent mesogloea. This suggests that they are due to electrotonic spread from the surface. In the preparation, almost no deflection was observed in the endoderm, implying that the endodermal positive phase and the slow negative phase of QSCPs have different origins.

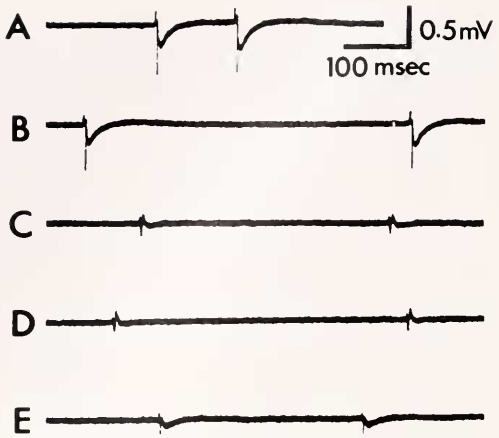

FIGURE 6. Amplitude changes of QSCPs associated with insertion depth of the recording electrode tip. Depth measurement was done with a single electrode. A, surface B, 40 μm; C, 90 μm; D, 190 μm; E, 290 μm.

Waveform changes of SMPs associated with electrode insertion depth

To permit SMPs to be triggered by lights-off stimulation, preparations were moderately anesthetized with 10^{-1} M urethane. Since this concentration did not immobilize animals completely, the experiment had to be done quickly. Initially, two electrode tips were placed a few mm apart from each other (not as in Figure 5, where they were placed directly side by side). The results are shown in Figure 7.

When both recording electrodes were placed on the surface of a radial streak, a pair of QSCPs and two pairs of SMPs appeared in both records (A). With the insertion of the electrode, very small negative deflections (B, upper trace) were seen. As the electrode was withdrawn the potentials reversed their polarity, increased in amplitude, and then became negative again, in a manner closely resembling Figure 5 (C–J). Similar results were obtained in 13 other experiments from seven animals. Positive pulses in the endodermal canal corresponded with QSCPs and SMPs and will be called PEPs. The maximum PEP was usually much larger than the maximum slow phase of QSCPs and the maximum SMP; in extreme cases without urethane treatment, the PEP reached about 4 mV, being four times larger than the corresponding SMP. The PEP sometimes showed a biphasic waveform with a negative phase, suggesting that it is a conducted event. It is noteworthy that QSCPs and SMPs together show coupling with PEPs, except for the last PEPs in D and E and the last SMP in the upper trace of J. These might have been lost in the course of conduction.

Pulses recorded form the ectoderm with high-resistance electrodes

When recording electrodes with resistances of 20–50 MΩ were placed on the surface of the radial streaks and brief vibrations were delivered by means of a jolting device (Tomita *et al.*, 1967), SMPs and the slow phase of QSCPs abruptly changed polarity immediately after a negative shift in the DC-level of 20–50 mV (mean, 37 mV; measurements were done in 12 cases). Large, positive, long duration pulses (ectodermal large pulses), amplitudes of which usually ranged

between 5 and 10 mV, were common in the 26 cases studied. They always corresponded either to SMPs or to the slow phase of QSCPs (Fig. 8A). It is quite clear that they originate in certain ectodermal cells of the radial streaks because the fine tips of electrodes used could not penetrate the opaque mesogloea without being damaged. To estimate membrane resistance changes during the large pulses, current pulses were delivered through a balanced bridge circuit but unexpectedly, no changes were observed in four cells measured (Fig. 8B). However, injection of positive current of about 10^{-8} A through the internal electrode often induced slow positive deflection similar to the ectodermal large pulses (Fig. 8D), resembling intracellularly recorded subthreshold pulses in the epithelio-muscular cell of *Nanomia* (Spencer, 1971). Pulses could not be evoked by delivering current extracellularly through such fine electrode tips. Even using electrodes with much larger tips of 20–30 μm, current of 10^{-5} A was needed. Furthermore, resistances were measured before and after withdrawal of the inserted electrode and a mean difference of 9.3 MΩ (variation, 3–4 MΩ) was obtained in five measurements. Therefore, it appears likely that the ectodermal large pulses are recorded within cells having an excitable membrane. Similarly, the experimental results indicate that SMPs and the slow phase of QSCPs originate in the same kind of cells and can therefore be regarded as extracellular forms of the ectodermal large pulses. The

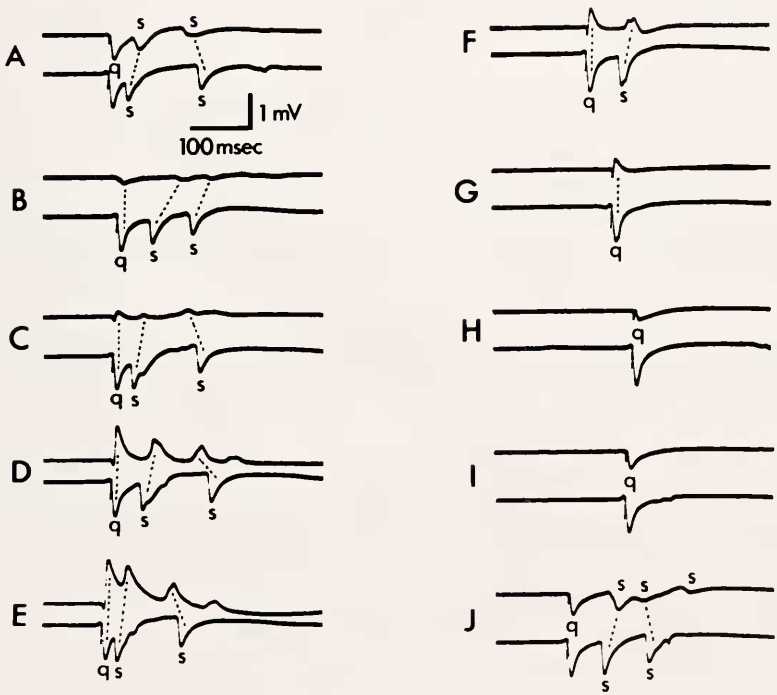

FIGURE 7. Waveform changes of SMPs (s) and QSCPs (q) associated with the depth of the recording electrode tip (upper trace). Lower trace is reference electrode on surface. A, surface; B, 460 μm; C, 360 μm; D, 310 μm; E, 210 μm; F, 110 μm; G, 60 μm; H, 40 μm; I, 20 μm J, surface. Originating sites of SMPs often changed; in the first pair of A they appeared first in the lower trace but in the second pair, the order was reversed. Dotted line shows possible pairs of pulses. All the pulses were evoked by terminating adapting light slightly before initiation of each recording.

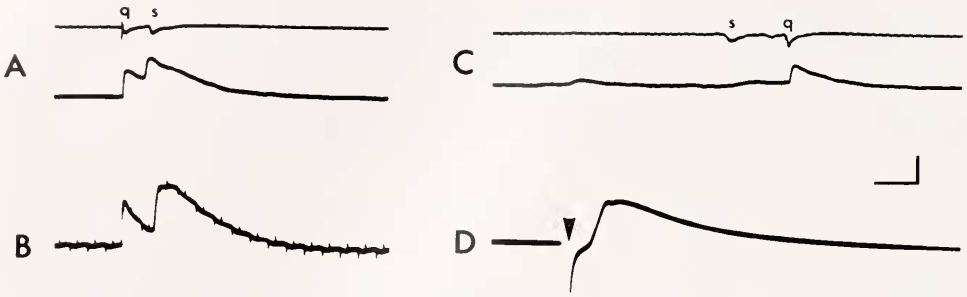

FIGURE 8. Intracellular recordings from ectoderm and endoderm. A: recording from the ectoderm of a radial streak with a high-resistance electrode (lower trace) and simultaneous extracellular recording from the ectodermal surface (upper trace), respectively. B: result of the resistance-change measurement. Current pulses with duration of 7 msec were delivered at 33 Hz. C: recordings from the endoderm of a radial streak with a high-resistance electrode (lower trace) and simultaneous extracellular recording from the ectodermal surface (upper trace). D: pulse evoked by electric current through a high-resistance electrode penetrating intracellularly in the ectodermal layer. Note the summation of ectodermal large pulses in A and B. Arrow: artifact due to current injection. Horizontal bar, 100 msec; vertical bar, 1 mV in the upper traces of A and C, 5 mV in B and the lower traces of A and C, 12.5 mV in D and 3.4 MΩ in B. q = QSCP, s = SMP.

two ectodermal large pulses occurring closely in time showed summation (Fig. 8A, B).

Pulses recorded from the endoderm with high-resistance electrodes

Since the fine tips of the high-resistance electrodes could not penetrate the opaque mesogloea, they were inserted into the endoderm of the radial streaks through cuts made at the bases of the tentacles. The insertion of electrodes with resistances of 80–100 MΩ sometimes resulted in positive pulses which were small, but somewhat larger than PEPs, showing amplitudes of 2–4 mV (Fig. 8C). Such pulses were obtained immediately after an abrupt negative shift of DC-level of 36–44 mV (mean, 40 mV in eight measurements). These pulses will be called endodermal large pulses. In Figure 8C, the SMP did not appear coupled with the endodermal large pulses because the inserted electrode was separated from the surface electrode by a distance greater than SMPs could travel, whereas in other records with shorter distances, SMPs and the endodermal large pulses often showed correspondence. Membrane resistance changes during the course of the endodermal large pulses could not be measured reliably because the high resistance of the electrodes resulted in unstable tip resistance. In one case where tip resistance was relatively stable, the resistance was measured before and after withdrawal of the inserted electrode and a difference of 13 MΩ was obtained, suggesting that the endodermal large pulses are also of intracellular origin.

DISCUSSION

QSCPs and SMPs rapidly increase in amplitude as the electrode is withdrawn to within 100 μm of the tissue surface and reach their maximum amplitudes at the ectodermal surface, suggesting that they are generated by ectodermal cells. A depth of 100 μm is greater than the thickness of the ectodermal layer (10–50 μm). The effects may be attributed to a current-guide effect of the hole made in the

tissues (especially in the opaque mesogloea) by the shank of the electrode during deep penetration.

The quick phase and the slow phase of QSCPs appear to have their origins in different cells, because the quick phase can be isolated using urethane (Fig. 4E). On the other hand, the slow phase of QSCPs and SMPs becomes smaller towards the nerve ring while the quick phase of QSCPs gets larger. This matches the histological observation that in this region, the muscle process of the myoepithelial cells become weaker and more nervous elements are observed. The slow phase of QSCPs and SMPs appear coupled with PEPs, and SMPs cannot usually cross over the groove between two radial streaks, where few myonal processes can be observed. This suggests that the muscle processes may generate the slow phase of QSCPs and SMPs; and the nervous elements, the quick phase of QSCPs. The latter seems more likely given the fact that the quick components have similar conduction velocities to pulses in the outer nerve-ring (nMPs, Ohtsu and Yoshida, 1973) and are usually coupled to them on a one-to-one basis. Indeed, a number of axons are observed among the myoepithelial cells.

It is not clear if SMPs are triggered events or not. Speculating from the fact that SMPs occur at lights-off, they seem to be triggered by something that could be described as a light-information carrier system. SMPs can also originate spontaneously without light stimuli. Non-nervous elements do not generally show repeated spontaneous firings, whereas SMPs do. Furthermore, extremely small deflections with very short duration were sometimes observed in the subtentacular region (Fig. 9A). It is likely, therefore, that those pulses trigger SMPs. However, recordings are not sufficient to permit definite conclusions. Another possibility is that conduction of SMPs is linked with the conducting system of PEPs.

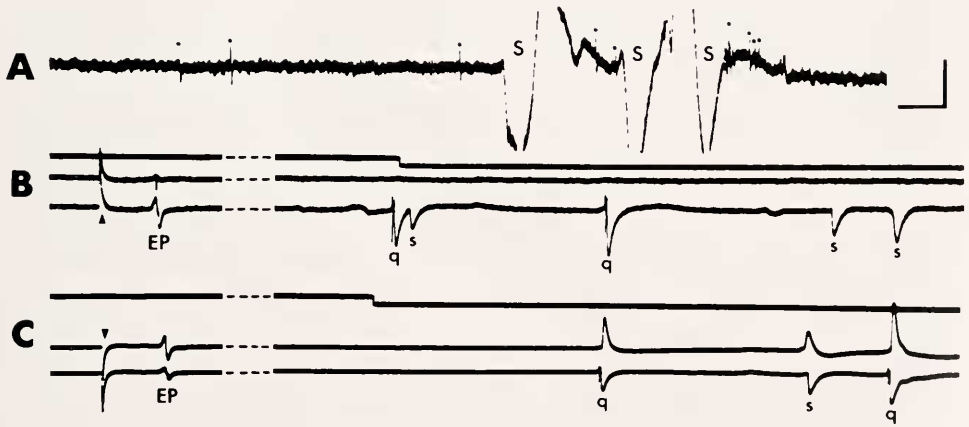

FIGURE 9. A: extremely small pulses (dots) recorded from the surface of a radial streak. B: simultaneous recordings from the exumbrellar epithelium near the ocelli (middle trace) and surface of a radial streak (lower trace). The first QSCP (q) and SMP (s) are spontaneous. Note: epithelial pulses (EPs) can invade into the radial streak, where they have longer durations and larger amplitudes than in the exumbrella, but QSCPs and SMPs are not conducted to the exumbrella. C: simultaneous recordings from the endoderm (middle trace) and the ectoderm (lower trace) of a radial streak. The PEPs (middle trace) appear coupled with the QSCPs and the SMPs. The EPs were evoked by a single shock of electrical stimuli (arrows) delivered to the exumbrella and the QSCPs and the SMPs were induced by lights-off (downward shifts of the upper traces in B and C). Horizontal bar, 100 msec, vertical bar, 0.1 mV in A, 0.4 mV in B and 1 mV in C.

Although intracellular dye-marking was not feasible, it appears from Figure 8 that the ectodermal large pulses are recorded intracellularly from the cells which also generate SMPs and the slow phase of QSCPs extracellularly. Histological investigations have revealed at least three types of cells—myoepithelial cells, nerve cells, and nematocytes—in the ectodermal layer of the subtentacular region. The latter two seem not to be responsible for generating the ectodermal large pulses because the region used for experiment includes only a small number of nematocytes, and neuronal somata large enough to be penetrated intracellularly are rare. Penetrations regularly showing the ectodermal large pulses would not be expected with so few cells. The epithelial processes of the myoepithelial cells, which cover almost all the subtentacular region, are therefore the most probable sites of origin of the ectodermal large pulses.

If the myoepithelial cell is penetrated by a micropipette electrode, then it is likely that the tip of the electrode usually lies in a large vacuole. This may explain why no resistance change is observed; the membrane of the vacuole, which might have a high resistance, impedes the resistance change occurring in the cytoplasmic membrane from reaching the inside of the vacuole.

Another possible reason for the lack of resistance changes is that some sensitive cells are actively excited while other, less sensitive ones receive passively conducted depolarizations spreading electronically from the former. The cell generating the ectodermal large pulses in Figure 8B might belong in the latter class, the loss of excitability being caused by the electrode impalement or some other factor. Electronic spread from other cells is possible if low-resistance intercellular pathways are present between the myoepithelial cells, as reported in other hydrozoan cells (Hand and Gobel, 1972; Mackie, 1976b; King and Spencer, 1979). Indeed, gap junctions are observed between muscle processes of *Spirocodon*.

When two pulses, whether QSCPs or SMPs, appear close together in time, summation is often observed in the ectodermal large pulses (Fig. 8A). This is reminiscent of the observation that closely spaced large QSCPs can evoke a TCP (Fig. 4D). The ectodermal large pulses, therefore, may develop into much larger action potentials inducing tentacular contraction when the membrane potential of the cell, probably the myoepithelial cell, is raised to a certain level (a critical depolarization potential) due to summation. This can be seen in the dissociated ectodermal epithelial cells of *Hydra*, in which spontaneous oscillations develop into large spikes (Kass-Simon and Diesl, 1977), and in the epitheliomuscular cell of the siphonophore *Nanomia*, where subthreshold pulses are thought to develop electrical responses with larger amplitude, causing twitch responses (Mackie, 1976a).

The mechanism generating PEPs is puzzling. The reversed polarity of PEPs and ectodermal slow pulses (Figs. 5, 7) suggests that the two are in a sink-and-source relationship in an electrogenerative system. Arguing against this idea is the long distance between the ectoderm, where SMPs (and the slow phase of QSCPs) are observed, and the central region of the endoderm, where the maximum PEPs are observed. Moreover, the opaque mesogloea between the ectoderm and the endoderm may function as a current barrier. The opaque mesogloea, however, is perforated in places with a tissue resembling an endodermal cell process, permitting endodermal cells direct contact with ectodermal cells. It is possible, therefore, that depolarizations of ectodermal cells reach electronically peripheral processes of endodermal cells and then are conducted electrogenerativly to the central region, generating PEPs.

The endodermal large pulses appear from Figure 8C to be recorded intracellularly from endodermal cells which also generate PEPs extracellularly. The small amplitude of the endodermal large pulses, however, argues against regarding them as intracellular recordings. The small amplitude is explicable if it is assumed (a) that the pulses recorded are due not to active excitation of the endodermal cells penetrated, but to electronic spread from other actively excited endodermal cells or (b) that recordings are from vacuoles.

PEPs sometimes show diphasic waveforms followed by negative deflections, suggesting that endodermal cells are excitable and conductive. If so, PEPs may be conducted back to ectodermal cells and cause small deflections. A similar case of endodermal pulses evoking pulses in ectodermal cells electrotonically has been reported in the siphonophore, *Nanomia* (Mackie, 1976a).

The pulses of *Spirocodon* are comparable to electrical potentials described in several hydrozoan medusae (*e.g.*, Mackie and Passano, 1968; Spencer, 1975; Mackie, 1975, 1976a; Spencer, 1978). As described above, the quick phase of QSCPs is best interpreted as a nervous event associated directly or indirectly with the outer nerve-ring, and the slow phase as an electrical concomitant of myoepithelial cell activity, triggered by the quick phase. In *Spiricodon* QSCPs (and SMPs) occurring singly are not usually accompanied by tentacular contractions, as far as can be observed under a dissecting microscope. This is different from *Proboscidactyla* (Spencer, 1975) but similar to *Sarsia* (Passano *et al.*, 1967). Tentacular contraction can be induced, however, when two pulses are close together in time, probably by summation or facilitation of two slow phases.

The slow phase of QSCPs decreases or disappears in excess Mg^{2+} and becomes larger stepwise by successive electrical stimuli, especially in a relatively depressed condition. In this respect, QSCPs obviously resemble the tentacle pulse (TP) in *Stomotoca* described by Mackie (1975); the quick phase appears to correspond to the pretentacle pulse (PTP) of Mackie (1975). Spencer (1978) has reported the TP without initial quick phase in the tentacles of *Polyorchis*. Also in *Spirocodon*, the quick phase was often extremely small, especially in tentacles, but QSCPs were readily distinguishable from SMPs and TCPs because the former was conducted only locally and the latter showed extremely slow conduction associated with muscle contraction.

Large specimens of *Spirocodon* with umbrellar diameter of 4–7 cm, as used in this study, show almost no crumpling in response to pricking the exumbrellar ectoderm with fine forceps. But such stimulation can evoke epithelial pulses (Ohtsu and Yoshida, 1973) similar to the CrPs of Spencer (1975, 1978). Small specimens of about 1 cm clearly show the crumpling response. Epithelial pulses distinct from SMPs and QSCPs (Fig. 9B, C) can also invade the subtentacular region, as in *Sarsia*. The pulses are larger in the endoderm than the ectoderm (Fig. 9C) but their generating origin remains to be investigated.

I should like to thank Professor G. O. Mackie of University of Victoria, Canada, and Dr. A. N. Spencer of University of Alberta, Canada, for their help in preparing this manuscript. Work supported in part by grants-in-aid to M. Yoshida from the Ministry of Education.

Summary

1. Three types of cells—myoepithelial cells, nerve cells, and nematocytes—are found in the ectoderm of the subtentacular region except near the nerve ring. A

single type of endodermal cell is identified in the endoderm of the subtentacular region except near the ring canal.

2. Three types of conductive pulses—QSCPs, SMPs, and TCPs—are recorded in the ectoderm. When recording electrodes are inserted into the endoderm, SMPs and the slow phase of QSCPs (negative pulses) are replaced by PEPs (positive pulses).

3. Using high-resistance electrodes, two types of pulses (ectodermal and endodermal large pulses) are recorded (presumably intracellularly) from the ectoderm and the endoderm, respectively. They probably originate in the myoepithelial cells and in the endodermal cells, respectively.

4. SMPs and the slow phase of QSCPs occur coupled with the ectodermal large pulses and appear to be generated in the same cells, as the extracellular forms of the latter. The quick phase of QSCPs is probably an event generated by nerves in the ectoderm.

5. PEPs occur coupled with the endodermal large pulses and may be generated in endodermal cells as the extracellular forms of the endodermal large pulses.

6. Pulses with extremely small amplitudes suggesting the presence of another conducting system can be recorded.

7. SMPs and QSCPs are different from the crumpling pulses of Spencer (1975).

LITERATURE CITED

Boelsterli, U., 1977. An electron microscopic study of early developmental stages, myogenesis, oogenesis and cnidogenesis in the anthomedusa, *Podocoryne carnea* M. Sars. *J. Morphol.*, **154**: 259–290.

Hand, A. R., and S. Gobel, 1972. The structural organization of the septate and gap junctions of *Hydra*. *J. Cell Biol.*, **52**: 397–408.

Horridge, G. A., 1955. The nerves and muscles of Medusae. II. *Geryonia proboscidalis* Eschscholtz. *J. Exp. Biol.*, **32**: 555–568.

Josephson, R. K., 1965. Three parallel conducting systems in the stalk of a hydroid. *J. Exp. Biol.*, **42**: 139–152.

Josephson, R. K., 1967. Conduction and contraction in the column of *Hydra*. *J. Exp. Biol.*, **47**: 179–190.

Josephson, R. K., 1974. Factors affecting muscle activation in the hydroid *Tubularia*. *Biol. Bull.*, **147**: 594–607.

Josephson, R. K., and M. Macklin, 1967. Transepithelial potentials in hydra. *Science*, **156**: 1629–1631.

Josephson, R. K., and G. O. Mackie, 1965. Multiple pacemakers and the behaviour of the hydroid *Tubularia*. *J. Exp. Biol.*, **43**: 293–332.

Josephson, R. K., and N. B. Rushforth, 1973. The time course of pacemaker inhibition in the hydroid *Tubularia*. *J. Exp. Biol.*, **59**: 305–314.

Kass-Simon, G., and V. K. Diesl, 1977. Spontaneous and evoked potentials from dissociated epithelial cells of *Hydra*. *Nature*, **265**: 75–77.

King, M. G., and A. N. Spencer, 1979. Gap and septate junctions in the excitable endoderm of *Polyorchis penicillatus* (Hydrozoa, Anthomedusae). *J. Cell Sci.*, **36**: 391–400.

Kruijf, H. A. M., 1977. Bursting pacemaker activity in the solitary hydroid *Tubularia solitaria*. *J. Exp. Biol.*, **68**: 19–34.

Mackie, G. O., 1975. Neurobiology of *Stomotoca*. II. Pacemakers and conduction pathways. *J. Neurobiol.*, **6**: 357–378.

Mackie, G. O., 1976a. The control of fast and slow muscle contractions in the siphonophore stem. Pp. 647–659 in G. O. Mackie, Ed., *Coelenterate ecology and behavior*. Plenum Press, New York.

Mackie, G. O., 1976b. Propagated spikes and secretion in a coelenterate glandular epithelium. *J. Gen. Physiol.*, **68**: 313–325.

Mackie, G. O., 1978. Coordination in physonectid siphonophores. *Mar. Behav. Physiol.*, **5**: 325–346.

Mackie, G. O., and L. M. Passano, 1968. Epithelial conduction in Hydromedusae. *J. Gen. Physiol.*, **52**: 600–621.

Mackie, G. O., and C. L. Singla, 1975. Neurobiology of *Stomotoca*. I. Action systems. *J. Neurobiol.*, **6**: 339–356.

Macklin, M., and R. K. Josephson, 1971. The ionic requirements of transepithelial potentials in *Hydra*. *Biol. Bull.*, **141**: 299–318.

Ohtsu, K., and M. Yoshida, 1973. Electrical activities of the anthomedusan, *Spirocodon saltatrix* (Tilesius). *Biol. Bull.*, **145**: 532–547.

Passano, L. M., and C. B. McCullough, 1962. The light response and the rhythmic potentials of hydra. *Proc. Nat. Acad. Sci. U. S. A.*, **48**: 1376–1382.

Passano, L. M., and C. B. McCullough, 1964. Co-ordinating systems and behaviour in *Hydra*. I. Pacemaker system of the periodic contractions. *J. Exp. Biol.*, 41: 643–664.

Passano, L. M., and C. B. McCullough, 1965. Co-ordinating systems and behaviour in *Hydra*. II. The rhythmic potential system. *J. Exp. Biol.*, **42**: 205–231.

Passano, L. M., G. O. Mackie, and M. Pavans de Ceccatty, 1967. Physiologie du comportement de l'hydroméduse *Sarsia tubulosa* Sars. Les systèmes des activités spontanées. *C. R. Acad. Sci. (Paris)*, **264**: 614–617.

Rushforth, N. B., 1971. Behavioral and electrophysiological studies of hydra. I. Analysis of contraction pulse patterns. *Biol. Bull.*, **140**: 255–273.

Rushforth, N. B., and D. S. Burke, 1971. Behavioral and electrophysiological studies of hydra. II. Pacemaker activity of isolated tentacles. *Biol. Bull.*, **140**: 502–519.

Singla, C. L., 1978. Fine structure of the neuromuscular system of *Polyorchis penicillatus* (Hydomedusae, Cnidaria). *Cell Tissue Res.*, **193**: 163–174.

Spencer, A. N., 1971. Myoid conduction in the siphonophore *Nanomia bijuga*. *Nature*, **233**: 490–491.

Spencer, A. N., 1975. Behavior and electrical activity in the hydrozoan *Proboscidactyla flavicirrata* (Brandt). II. The medusa. *Biol. Bull.*, **149**: 236–250.

Spencer, A. N., 1978. Neurobiology of *Polyorchis*. I. Function of effector systems. *J. Neurobiol.*, **9**: 143–157.

Spencer, A. N., 1979. Neurobiology of *Polyorchis*. II. Structure of effector systems. *J. Neurobiol.*, **10**: 95–117.

Toh, Y., M. Yoshida, and H. Tateda, 1979. Fine structure of the ocellus of the hydromedusan, *Spirocodon saltatrix*. I. Receptor cells. *J. Ultrastruct. Res.*, **68**: 341–352.

Tomita, T., A. Kaneko, M. Murakami, and E. L. Pautler, 1967. Spectral response curves of single cones in the carp. *Vision Res.*, **7**: 519–531.

Uchida, T., 1927. Studies on Japanese Hydromedusae. I. Anthomedusae. *J. Fac. Sci. Imp. Univ. Tokyo, Section IV*, **1**: 145–241.